
Article:
Mason, J, Henry, A orcid.org/0000-0002-5379-6618 and Bownes, P (2020) Error detection thresholds for routine real time in vivo dosimetry in HDR prostate brachytherapy. Radiotherapy and Oncology. ISSN 0167-8140

https://doi.org/10.1016/j.radonc.2020.04.058

Error detection thresholds for routine real time in vivo dosimetry in HDR prostate brachytherapy

Josh Mason[a,b], Ann Henry[a,c], Peter Bownes[a],

a - Leeds Cancer Centre, Leeds, UK

b – Currently at Imperial College Healthcare NHS Trust, London, UK

c - University of Leeds, UK

Corresponding author:

Josh Mason

Department of Radiation Physics and Radiobiology

Charing Cross Hospital

Imperial College Healthcare NHS Trust

London W6 8RF

United Kingdom

44 113 20 67905

joshua.mason@nhs.net

Keywords: In vivo dosimetry; prostate brachytherapy

This manuscript is fifteen pages including title page, summary and references. There are also three figures and three tables.

Purpose Routine real time in vivo dosimetry (IVD) is performed in HDR prostate brachytherapy to independently verify dose delivery. This study investigates impact of position uncertainty on error detection thresholds for IVD.

Methods IVD is implemented using a microMOSFET placed centrally in the prostate using an additional needle. 144 IVD measurements were made for 15Gy or 19Gy single fraction treatments. Needle insertion and treatment planning used real-time trans-rectal ultrasound. Source-MOSFET position thresholds of ±1, ±2 and ±3mm were used to calculate per-needle and total plan error detection thresholds for the measured dose using an uncertainty analysis based on the treatment plan data.

Results The median dose difference from 144 total plan measurements was -5.2% (range +7.4% to -17.3%). 3 plans measured outside the total plan error detection threshold for position threshold ±1mm, no plans measured outside the total plan error detection threshold for larger position thresholds. For 2233 individual needle measurements, for position thresholds of ±1mm, ±2mm and ±3mm the number of needles outside the per-needle error detection threshold was 103, 25 and 10 respectively and the number of treatments that would have required interruption based on these thresholds for real-time IVD was 66, 16 and 8 respectively.

Conclusion IVD in HDR prostate brachytherapy using a microMOSFET provides a high level of confidence that we are correctly delivering the planned dose to our patients. A ±2-3mm position threshold gives an appropriate balance between error detection and avoiding unnecessary treatment interruptions.

Introduction

In high dose rate (HDR) prostate brachytherapy metal or plastic needles are implanted into the prostate gland through the perineum and the treatment is delivered using a single radioactive source driven by a remote afterloader. The dwell positions where the source stops within each needle, and the dwell time that the source stops at each dwell position, are optimised to deliver the required dose to the prostate gland while reducing the dose to organs at risk and surrounding normal tissue as much as possible. This allows HDR prostate brachytherapy treatments to deliver large single fraction doses, for example 15 Gy or 19 Gy [1]. UK guidance recommends that in vivo dosimetry (IVD) should be in routine use for most patients at the beginning of treatment [2]. It follows that IVD should be performed for this patient group, however IVD is not commonly performed in brachytherapy treatments for several reasons including limited availability of suitable commercial detectors, difficulty of access to the treatment site and maintaining the detector in a stable position during treatment, steep dose gradients requiring small detectors and increasing the impact of position uncertainty and temperature and energy dependence of detector response [3]. Errors in HDR prostate brachytherapy treatments that could be detected by IVD, with reference to Table 1 in the Vision 20/20 paper by Tanderup et al [3] include afterloader malfunction, intra/interfraction needle motion, needle reconstruction errors, applicator/source index length setting errors, interchanged transfer tubes and treatment planning system (TPS) dose calculation related errors (for example incorrect source data selection).

Especially for single fraction treatments, IVD should be performed in real-time to allow errors to be detected, treatment interrupted and corrective action to be taken before treatment is completed. This requires appropriate error detection thresholds that will allow significant errors to be detected while minimising the number of false errors declared by the IVD system as unnecessary treatment interruptions must be minimised for patients under general anaesthetic. Our previous study demonstrated that position uncertainty has a large impact on error detection thresholds due to high dose

gradients in brachytherapy treatments [4]. This study investigates the impact of different position thresholds on the number of potential errors that would require treatment interruptions using retrospective IVD data from a large cohort of HDR prostate brachytherapy patients.

Method

Patient group and HDR treatments

144 IVD measurements were performed between July 2014 and August 2019. Treatments were single fraction boost followed by 37.5 Gy in 15 fractions of external beam to the prostate and seminal vesicles or single fraction monotherapy/salvage. Plans were prescribed to the prostate D_{90}, with 15 Gy and 19 Gy to the 100% isodose levels for boost and monotherapy/salvage treatments respectively. All patients were planned using a trans-rectal ultrasound (TRUS) guided real-time approach where needle insertion, treatment planning and treatment delivery are done under TRUS guidance in a single dedicated HDR theatre with the patient under general anaesthetic and in the lithotomy position throughout so there is no movement of the patient between treatment planning and delivery.

Treatments were delivered using a Flexitron Ir-192 afterloader (Elekta AB, Stockholm, Sweden) and stainless steel needles (interstitial bevel needle product number 083.045, Elekta AB). Needles were inserted approximately 1 cm apart around the periphery of the prostate with 2-5 needles inserted more centrally for dose coverage of the base and apex of the gland. Needles were inserted using a template that is locked before acquisition of TRUS images for treatment planning. Dwell positions were activated throughout the PTV (PTV = prostate + 3 mm, 0 mm posteriorly) with 2 mm spacing. Plan objectives were prostate $V_{100} > 95\%$, PTV $V_{100} > 95\%$. Constraints were urethra $D_{10} < 17.5$ Gy and rectum $D2cm^3 < 11.8$ Gy, $V_{100} = 0$ cc for boost [5] and urethra $D_{10} < 22$ Gy, $D_{30} < 20.8$ Gy, $V_{150} = 0$ cc and rectum $D2cm^3 < 15$ Gy, $V_{100} = 0$ cc for monotherapy [6].

MOSFET calibration and commissioning

IVD is implemented using a microMOSFET (model TN-502RDM-H Best Medical, Ottawa, Canada, hereafter referred to as MOSFET). The MOSFET is calibrated at the centre of a perspex phantom with a source-MOSFET distance of 1cm [4]. The MOSFET sensitivity factor is determined from the ratio of the MOSFET reading to the expected dose calculated using Monte Carlo (MC) simulation of the phantom geometry [4,7]. Other MOSFET commissioning measurements showed no corrections were required for linearity, anisotropy, temperature dependence within the measurement uncertainty, however a correction 2.6% cm^{-1} increase in MOSFET relative response with increasing source-MOSFET distance is required to account for MOSFET energy dependent response [4].

IVD implementation

For this method, and throughout this study, mV is used as a surrogate for delivered dose as it allows the MOSFET readout to be directly compared to dose prediction without any conversion to Gy being required. The predicted MOSFET accumulated mV reading is calculated using data exported from the treatment planning system (Oncentra Prostate, Elekta AB), by multiplying each individual dwell position's planned dose contribution (calculated by the treatment planning systems implementation of TG-43 formalism) to the measurement point by the MOSFET mV/Gy sensitivity factor and applying the energy dependent response correction based on the distance between each individual dwell position and the MOSFET. The prediction includes a correction for attenuation of dose by the steel needles [4]. Per-needle and total plan predicted readings are calculated by summing the individual dwell position contributions. Figure 1 shows an example transverse slice from a treatment plan indicating a typical position for the MOSFET detector.

The MOSFET is inserted in an additional needle placed as close to the centre of the prostate as possible (while avoiding the urethra), this minimises the dose gradient at the measurement point as due to the peripheral loading technique used, the dwell weight is around the periphery of the prostate gland. The MOSFET is fixed with tape and a mark is made on the MOSFET cable to ensure it is inserted to the correct depth – usually mid-gland. After the treatment has been delivered the MOSFET position is reviewed to ensure it hasn't moved. During treatment the MOSFET reading is recorded before and after delivery of each needle using the in room camera to monitor the MOSFET reader, allowing the mV per needle to be calculated as each needle is delivered. Each MOSFET has a lifetime accumulated mV limit of 20,000 mV so typically ~10 patients can be measured with a single MOSFET.

Error detection thresholds

Error detection thresholds were determined on a per needle and per plan basis using a full uncertainty analysis as recommended by Kirisits et al [8]. Table 1 lists the uncertainty components and an example uncertainty calculation is included in supplementary material of our previous publication [4]. The error detection threshold is the k=2 uncertainty value for all the uncertainty components listed in Table 1, combined in quadrature and the result multiplied by 2.

The position uncertainty in Table 1 is estimated by applying a position threshold. The position threshold is the distance below which we do not wish to detect position errors, for example due to limits on reconstruction accuracy or because we believe errors below a certain level are not clinically significant. The position uncertainty is calculated using an inverse-square law approximation to estimate the dosimetric impact of a shift in the source-MOSFET relative position of ±the position threshold. This is estimated for each dwell position and a weighted average (weighted on the dose contribution from each dwell position) is used to estimate the overall

uncertainty for each needle/plan. In this study uncertainties were calculated separately and the analysis repeated for position thresholds ±1 mm, ±2 mm and ±3 mm to investigate the impact of position threshold on the number of needles/plans exceeding the error detection threshold.

For each needle and plan the measured – predicted mV was retrospectively compared to the error detection threshold to check for potential errors. The analysis was repeated for each of the position thresholds (±1 mm, ±2 mm and ±3 mm).

Results

Figure 2 shows a measurement for one patient with two needles outside the error detection threshold. Figure 3(a) shows the relative contributions of individual dwell positions to the total plan dose calculated from 5 randomly selected patient measurements, illustrating that in most cases the MOSFET dose is not dominated by individual dwell positions. The large number of dwells with low contribution is due to the peripheral loading technique resulting in large numbers of dwells with low or zero weight in the centre of the prostate. Note that Figure 3(a) shows the dwell contributions to the dose at the MOSFET position, dependent on both dwell time and distance from the MOSFET, not the overall plan distribution of dwell time weighting. Figure 3(b) shows the relative contributions of individual needles to the total plan dose across all 144 patients. Again this represents contribution to dose at the MOSFET position and illustrates that in most cases the MOSFET dose is not dominated by a single needle. This is achieved by positioning the MOSFET close to the centre of the prostate. This was not always possible and there was one extreme case in the measurement of a focal salvage case where the MOSFET was positioned close to a heavily weighted dwell position, where a single dwell <3mm from the MOSFET contributed 15% of the per-needle dose, and that needle contributed 46% of the total plan dose. Focal salvage cases are more difficult to measure – because only a sub-volume of the prostate usually excluding the urethra is treated, there is no

need to reduce dose in the centre of the implant and the needle density in the implant is greater than for whole gland treatments. This same case also accounts for the very large values for the per-needle uncertainty shown in Table 2.

The median difference between measured and predicted mV from 144 total plan measurements was -5.2% (range +7.4% to -17.3%) (measured - predicted). For ±1 mm position threshold the median error detection threshold was ±12.1% and 8/144 plans measured outside the error detection threshold. In 5/8 of these cases all needles in the plan passed the individual needle error detection threshold and on reviewing these cases it was found that one very heavily weighted needle caused the overall plan measurement to fail even though that needle was within its error detection threshold, demonstrating a limitation of the statistical model. In such cases the plan measurement exceeding the error detection threshold could be ignored leaving 3/144 plan measurements outside the error detection threshold with median difference -14.6% (range -13.5% to -15.8%). For ±2 mm and ±3 mm position threshold all 144 plans passed.

For 2233 needle measurements, the median difference between measured and predicted mV was -5.7% (range +633% to -129%) (measured - predicted). For a position threshold of ±1mm 103/2233 needles exceeded the error detection threshold calculated individually for each needle, affecting 66/144 patient treatments. For position threshold of ±2mm this reduced to 25/2233 in 16/144 patient treatments and for position threshold of ±3mm this further reduced to 10/2233 in 8/144 patient treatments. Table 2 summarises the needles that exceeded the error detection threshold for each position threshold value, with separate results presented based on the magnitude of the difference between measured and predicted reading to indicate the magnitude of the dosimetric differences detected at the MOSFET position. Table 2 also shows the median weighted distance for the needles that exceeded the error detection threshold in each category, this is the average of the distances between the MOSFET and each source position

in the needle, weighted by the contribution of that source position to the total dose measured at the MOSFET position for that needle.

Needle measurements that exceeded the error detection threshold for ±1mm position threshold and had an absolute difference of >25mV (~0.25Gy) were reviewed by looking back at the original treatment plan data. The results are summarised in Table 3 and discussed further in the Discussion section.

Discussion

This study has investigated application of error detection thresholds for real time IVD in HDR prostate brachytherapy using a microMOSFET, with the objective of defining an error detection threshold that allows an error to be detected for an individual needle, so that treatment can be interrupted and the cause of error investigated and corrected before continuing the treatment. An error detection threshold is also defined for the total plan measurement, this would not enable treatment interruption but could be used to flag cases where further investigation should be performed at the end of treatment, for example re-acquiring images to check needle positions. The results of such investigations would still benefit patients by informing future practice.

Choice of position threshold

The error detection threshold is calculated from an uncertainty analysis including all components of uncertainty but due to the high dose gradient inside a HDR prostate implant position uncertainty dominates. Therefore the error detection threshold depends on the position threshold that is used in the uncertainty analysis – the acceptable level of deviation in the relative position of the source dwell positions and the MOSFET. In this study position thresholds of ±1mm, ±2mm and ±3mm were investigated. This retrospective review was performed to determine which position threshold would result in an error detection threshold sensitive enough to detect true

errors but reduce false positives that would lead to unnecessary treatment interruptions, with potentially adverse impact for a patient under general anaesthetic. The results of this study show that the choice of position threshold is crucial for this decision making as the number of interruptions that would have been required varied between almost half of all treatments for position threshold of ±1mm to ~5% for position threshold of ±3mm.

Determining clinical significance of results

In choosing a position threshold it is important to minimize unnecessary treatment interruptions but the clinical significance of deviations in position also must be considered. This has been investigated by Poder et al [9] who simulated source position errors in HDR prostate plans and found that the position thresholds required to prevent clinically significant changes in prostate DVH statistics could be 2-5mm depending on direction of the error, dwell weight and needle position within the prostate, with a similarly complicated situation for OAR constraints. Buus et al [10] concluded that a 2mm needle migration threshold might be necessary for single fraction treatments of 15Gy or more, in a study based on actual observed needle movement, albeit in MRI based planning which is slightly different from a TRUS based workflow where the patient isn't moved between insertion and treatment. These studies illustrate that it is not possible to determine an absolute position threshold for clinical significance and instead the position threshold should be chosen to allow potentially clinically significant errors to be detected while accepting that this will result in some unnecessary treatment interruptions. If a measurement exceeds the error detection threshold it is a limitation of the method using a single point IVD measurement that it is not possible to determine the clinical impact from the measurement alone. For example if the dose for a single needle is lower than expected then it can be concluded that the needle has moved away from the MOSFET but the new position of the needle can't be determined exactly. Instead it would be necessary to review the treatment plan data and possibly acquire a new set of imaging data to try to determine the clinical impact. These limitations could be addressed by increasing the number of

points of measurement but this would also introduce more complexity into the IVD process. Alternative approaches to brachytherapy verification that track the source position as it moves would allow the impact on overall treatment to be reconstructed more easily but have the disadvantage of not measuring dose directly [11,12].

Which needles are outside the error detection threshold?

Table 2 summarises the needles which measured outside the error detection threshold. A significant proportion are small differences (0 - 25mV which is approximately 0 -25cGy) in needles that have low predicted readings. A low predicted reading can be due to the needle having low dwell weighting in the plan or being distant from the MOSFET. Table 2 shows that on average the needles with low predicted readings are not a much greater distance from the MOSFET than other needles, so it is likely that the majority of these detected errors are due to a limitation in the uncertainty calculation not properly taking account of random variation in the MOSFET response for low mV/low dose readings. A further limitation of using a single point of measurement is that it restricts the ability to detect errors in needles that are furthest from the MOSFET – these may contribute a low dose to the MOSFET but still be clinically significant in the plan. However positioning the MOSFET as close as possible to the centre of the prostate should mean that in most cases the MOSFET is able to detect errors in all needles that have significant weight in the plan. Table 2 illustrates that across the range of mV differences the needles are similar in terms of percentage difference between measured and predicted reading, and distance from the MOSFET, although the small number of needles with very large mV differences tend to be closer to the MOSFET as would be expected. Similarly Figure 3 (b) illustrates that there are only a small number of cases where a single needle dominates the MOSFET response.

The needles exceeding the error detection threshold with difference >25mV were investigated by reviewing the original plan data. Some could be explained by errors in MOSFET/needle reconstruction caused by poor

TRUS image quality. The reconstruction errors were small (<2mm) as demonstrated by the fact that these needles did not exceed the error detection threshold when position threshold was increased above ±1mm. Some needles were in the posterior of the prostate and previous work comparing treatment planning TRUS to images acquired just after treatment has shown these needles tend to drop [4], possibly due to resolving haematoma. A number of the needles exceeding the error detection threshold were in the most lateral positions which tend to be the hardest needles to confidently identify in the TRUS image and are sometimes placed on the edge of the prostate capsule which could make movement more likely. Some of the needles were centrally placed which in a peripheral loading technique means that the needles are heavily weighted at the base and apex of the prostate with zero dwell weight at mid-gland close to the MOSFET. Discrepancies for these needles could be due to angular dependence in MOSFET response that was not picked up at commissioning**.** Finally in one case, at treatment a needle was found to have slipped back in the template by 3mm, treatment continued as it was calculated that this would not cause a clinically significant impact on the treatment plan but the dose difference was sufficient to exceed the error detection threshold.

Position uncertainties were higher than estimated by Kertscher et al [13] using random position error simulations who found k=1 position uncertainties up to 15.9%, lower than found in this study, however the closest source-detector position was 6 mm compared to 2.7 mm in this study. Some very large uncertainties in this study were due to the MOSFET being positioned very close to a heavily weighted needle; this could be avoided by more careful positioning of the MOSFET however it can be difficult to avoid placing the MOSFET close to a treatment needle when the prostate is small.

Overall measurements were systematically low compared to prediction by ~5%. In our previous study images acquired after treatment showed on average ~2% dose reduction at MOSFET position due to the tendency for

the posterior row of needles to drop [4]. The correction for MOSFET energy dependent response is assumed to be linear with distance, however a recent study by Van Gellekom et al [14] found that at 5mm distance the MOSFET relative response changes non-linearly which if correct would reduce the predicted readings in our study, however it is very difficult to accurately measure the relative response at small distances due to the dose gradient around the source. A further possible explanation for measuring systematically low is limitation in the accuracy of planning on ultrasound in terms of reconstruction accuracy. A study by Carrara et al [15] using detectors in the rectum during 18 prostate HDR treatments found an average difference between measured and predicted dose of -2.1%, and in common with our previous study, also observed better agreement to the dose reconstructed on images acquired after treatment.

Overall IVD measurements give good agreement considering the large uncertainties involved and provide a high level of confidence that we are correctly delivering the planned dose to our patients. In common with other IVD methods, it is difficult to completely avoid declaring false errors when defining error detection thresholds for real-time per needle IVD. The results of this analysis can be used to achieve a balance between frequency of treatment interruption and the need to detect errors in real-time IVD. A position threshold of 2-3 mm is suitable to achieve this.

Table 1 Results of the uncertainty analysis. For variable uncertainty components the values shown are the median with the minimum and maximum values in parentheses.

Description	Type	Position[a] threshold	Per needle uncertainty	Total plan uncertainty
MOSFET calibration (k=1)[b]	A		2.7 %	2.7 %
Energy correction (k=1)[b]	A		1.7 %	0.3 %
Angular dependence (k=1)[b]	A		3 %	0 %
Source calibration (k=1)[c]	A		2 %	2 %
TPS dose calculation (k=1)[c]	B		3 %	3 %
Median (min, max) position uncertainty (k=1)[a]	B	±1 mm	11.2% (2.8%, 76.8%)	4.0% (0.9%, 7.5%)
		±2 mm	23.8% (5.7%, 394%)	8.9% (1.9%, 22.0%)
		±3 mm	38.1% (8.7%, 538%)	15.9% (2.9%, 208%)
Median (min, max) MOSFET reproducibility (k=1)[b]	A		3.4% (0.8%, 47%)	0.4% (0.3%, 0.5%)
Median (min, max) total uncertainty (k=2)		±1 mm	28.9 % (13.6%, 207%)	12.1 % (9.3%, 17.5%)
		±2 mm	51.9 % (18.5 %, 789%)	20.0 % (9.8%, 44.9%)
		±3 mm	79.3 % (23.9 %, 1076%)	33.1 % (10.8%, 416%)

[a]The impact of position uncertainty on the predicted dose measurement is estimated using an inverse square law approximation applying the position threshold to the MOSFET-source distances within each needle.

[b]Taken from Mason et al [4].

[c]Taken from Kirisits et al [8].

Table 2 Summary of the needles outside the error detection threshold categorised by magnitude of the difference between measured and predicted mV. Note that 100mV is approximately 1 Gy. Separate results are presented for the different position threshold values used in the error detection threshold calculation.

Magnitude of difference between measured and predicted mV	Number of needles	Median Predicted reading (mV)	Median difference as % of predicted mV	Median error detection threshold	Median weighted distance (cm)[a]
Position threshold = ±1mm[b]					
All	103	57.1	37%	±28%	2.17
0 mV – 10 mV	20	13.2	56%	±41%	2.28
10 mV – 25 mV	51	51.9	30%	±25%	2.19
25 mV – 50 mV	26	83.3	40%	±24%	1.97
50 mV – 100 mV	5	164	37%	±27%	1.74
100 mV – 200 mV	1	274	46%	±46%	0.95
Position threshold = ±2mm[b]					
All	25	15.7	67%	±46%	2.54
0 mV – 10 mV	10	9.95	80%	±58%	2.28
10 mV – 25 mV	5	15.7	74%	±58%	1.74
25 mV – 50 mV	9	75.1	44%	±33%	2.75
50 mV – 100 mV	1	79.8	70%	±32%	2.9
100 mV – 200 mV	0	-	-	-	-
Position threshold = ±3mm[b]					
All	10	8.5	111%	±68%	2.21

0 mV – 10 mV	5	5.17	124%	±77%	2.05
10 mV – 25 mV	3	32.2	70%	±61%	2.22
25 mV – 50 mV	2	62.2	129%	±43%	2.91
50 mV – 100 mV	0	-	-	-	-
100 mV – 200 mV	0	-	-	-	-

[a] For each needle, the weighted distance is average of the distances between the MOSFET and each source position in the needle, weighted by the contribution of that source position to the total dose measured at the MOSFET position for that needle.

[b] The impact of position uncertainty on the predicted dose measurement is estimated using an inverse square law approximation applying the position threshold to the MOSFET-source distances within each needle.

Table 3 Needles that measured outside the error detection threshold and had an absolute difference between measured and predicted reading of >25mV were investigated and this table shows the number within each category from the investigation.

Position threshold	±1 mm	±2 mm	±3 mm
MOSFET/needle reconstruction errors	7	0	0
Posterior needles	8	0	0
Lateral needles	7	4	1
Central needles	5	5	1
Needle movement	1	0	0
Unexplained	4	1	0

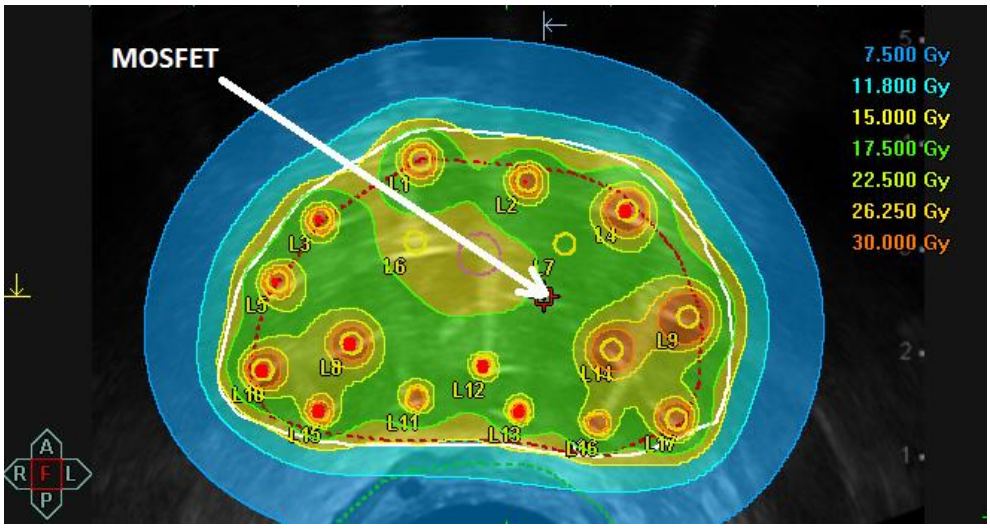

Figure 1 Central slice from a typical treatment plan. The MOSFET position is indicated by the white arrow. Measurement results for this plan are shown in Figure 2. Needles 14 and 17 measurements were outside the error detection threshold for position threshold of ±1mm. The plan is prescribed to prostate D90 of 17.1 Gy.

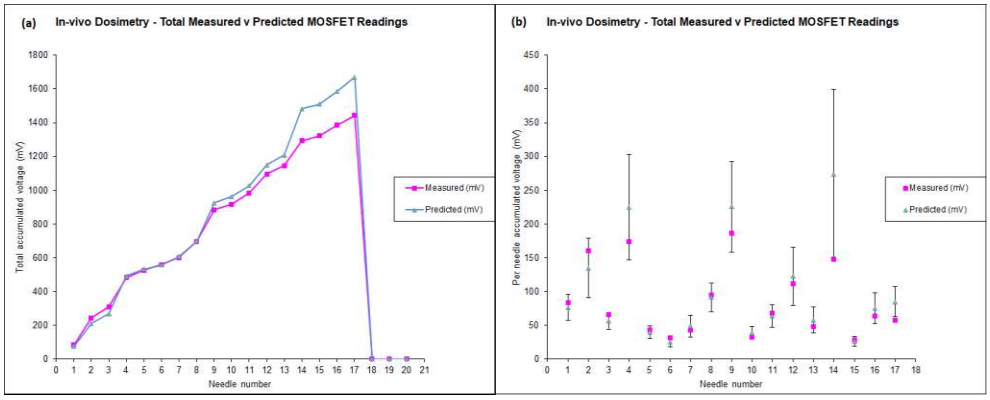

Figure 2 Measured versus predicted MOSFET readings for the patient whose treatment plan is illustrated in Figure 1, (a) the total accumulated reading as the plan is delivered (b) the individual needle measurements and predicted readings with error bars showing the k=2 error detection thresholds calculated for position threshold of ±1mm. Needles 14 and 17 measurements were outside the error detection threshold. These results could be explained by an error in reconstruction of the MOSFET position and were inside the error detection threshold for position threshold of ±2mm.

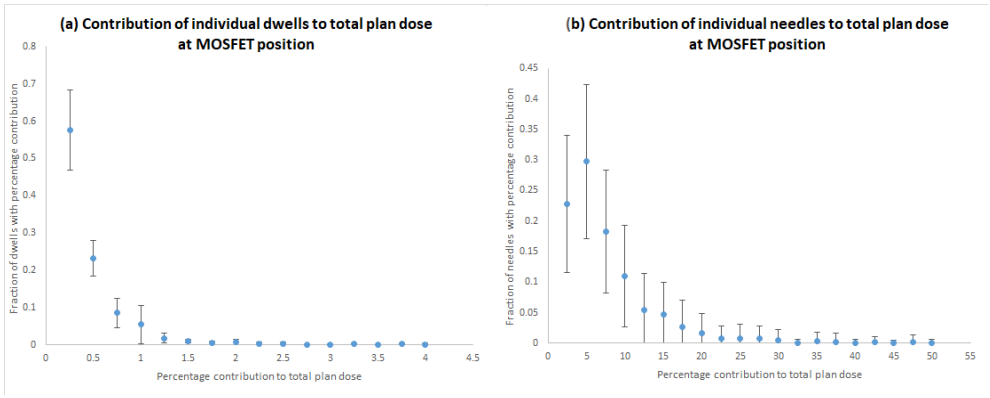

Figure 3 (a) The fraction of individual dwell positions that contribute a certain percentage to the total plan dose measured at the MOSFET position. Values are the mean across five randomly selected patients and the error bars the standard deviation. Each data point represents a range, for example the fraction of dwells with percentage contribution 0.25% includes the range 0 to 0.25%, the fraction for 0.5% includes the range 0.25% to 0.5% and so on. (b) The fraction of individual needles that contribute a certain percentage to the total plan dose measured at the MOSFET position. Values

are the mean across all patients and the error bars the standard deviation. The percentage contribution values represent a range as for (a).

REFERENCES

[1] Hoskin PJ, Colombo A, Henry A, et al. GEC/ESTRO recommendations on high dose rate afterloading brachytherapy for localised prostate cancer: An update. Radiotherapy and Oncology 2013;107:325-332.

[2] Donaldson S. Towards safer radiotherapy. British Institute of Radiology, Institute of Physics and Engineering in Medicine, National Patient Safety Agency, Society and College of Radiographers, The Royal College of Radiologists, London 2007.

[3] Tanderup K, Beddar S, Andersen CE, Kertzscher G Cygler JE. In vivo dosimetry in brachytherapy. Medical physics 2013;40:070902.

[4] Mason J, Mamo A, Al-Qaisieh B, Henry AM Bownes P. Real-time in vivo dosimetry in high dose rate prostate brachytherapy. Radiotherapy and Oncology 2016;120:333-338.

[5] Morton G, Loblaw A, Cheung P, et al. Is single fraction 15Gy the preferred high dose-rate brachytherapy boost dose for prostate cancer? Radiotherapy and Oncology 2011;100:463-467.

[6] Hoskin P, Rojas A, Ostler P, et al. High-dose-rate brachytherapy alone given as two or one fraction to patients for locally advanced prostate cancer: Acute toxicity. Radiotherapy and Oncology 2013.

[7] Mason J, Al-Qaisieh B, Bownes P, Thwaites D Henry A. Dosimetry modeling for focal high-dose-rate prostate brachytherapy. Brachytherapy 2014.

[8] Kirisits C, Rivard MJ, Baltas D, et al. Review of clinical brachytherapy uncertainties: Analysis guidelines of GEC-ESTRO and the AAPM. Radiotherapy and Oncology 2014;110:199-212.

[9] Poder J, Carrara M, Howie A, et al. Derivation of in vivo source tracking error thresholds for TRUS-based HDR prostate brachytherapy through simulation of source positioning errors. Brachytherapy 2019; 18:711-719.

[10] Buus S, Lizondo M, Hokland S, et al. Needle migration and dosimetric impact in high-dose-rate brachytherapy for prostate cancer evaluated by repeated MRI. Brachytherapy 2018; 17:50-58.

[11] Nose T, Chatani M, Otani Y, et al. Real-Time Verification of a High-Dose-Rate Iridium 192 Source Position Using a Modified C-Arm Fluoroscope. International Journal of Radiation Oncology, Biology and Physics 2017; 97:858-865.

[12] Smith R, Hanlon M, Panettieri V, et al. An integrated system for clinical treatment verification of HDR prostate brachytherapy combining source tracking with pretreatment imaging. Brachytherapy 2018; 17:111-121.

[13] Kertzscher G, Andersen CE, Siebert FA, Nielsen SK, Lindegaard JC Tanderup K. Identifying afterloading PDR and HDR brachytherapy errors using real-time fiber-coupled Al2O3:C dosimetry and a novel statistical error decision criterion. Radiotherapy and oncology 2011;100:456–462.

[14] Van Gellekom MP, Canters RA, Dankers FJ, Loopstra A, van der Steen-Banasik EM Haverkort MA. In vivo dosimetry in

gynecological applications—A feasibility study. Brachytherapy 2018;17:146-153.

[15] Carrara M, Tenconi C, Rossi G, et al. In vivo rectal wall measurements during HDR prostate brachytherapy with MOSkin dosimeters integrated on a trans-rectal US probe: Comparison with planned and reconstructed doses. Radiotherapy and Oncology 2016;118:148-153.